

Dynamical Particle-Hole Asymmetry in High-Temperature Cuprate Superconductors

B. Sriram Shastry

Department of Physics, University of California, Santa Cruz, California 95064, USA

(Received 5 October 2011; published 10 August 2012)

Motivated by the form of recent theoretical results, a quantitative test for an important dynamical particle-hole asymmetry of the electron spectral function at low energies and long wavelengths is proposed. The test requires the decomposition of the angle resolved photo emission intensity, after a specific Fermi symmetrization, into odd and even parts to obtain its ratio \mathcal{R} . A large magnitude \mathcal{R} is implied in recent theoretical fits at optimal doping around the chemical potential, and I propose that this large asymmetry needs to be checked more directly and thoroughly. This processing requires a slightly higher precision determination of the Fermi momentum relative to current availability.

DOI: [10.1103/PhysRevLett.109.067004](https://doi.org/10.1103/PhysRevLett.109.067004)

PACS numbers: 74.72.-h, 74.20.Mn, 74.25.Jb

Introduction.—The search for a microscopic theory of the normal state of the cuprates is one of the main themes in condensed matter physics for the last two decades. The recent suggestions of describing the normal state in terms of theories with a quantum critical point [1] have also created wide interest in other branches of physics such as string theory and quantum gravity [2]. An initial theoretical objective is the derivation of the normal state low energy long wavelength single electron spectral function $\rho_{\mathcal{G}}(\vec{k}, \omega)$ [or equivalently $A(\vec{k}, \omega)$], encoding the complete set of symmetries.

In this Letter, I discuss the behavior of $\rho_{\mathcal{G}}(\vec{k}, \omega)$ under a dynamical particle-hole transformation simultaneously inverting the wave vector and energy relative to the chemical potential μ as

$$(\vec{k}, \omega) \rightarrow -(\vec{k}, \omega), \quad \text{with} \quad \vec{k} = \vec{k} - \vec{k}_{\text{F}}. \quad (1)$$

Invariance under this transformation has often been invoked in analyzing angle resolved photoemission (ARPES) data [3]. It is an emergent symmetry of the Fermi-liquid in the sense of Ref. [4], arising when correction terms of $O(\omega/\varepsilon_{\text{F}})^3$ are neglected [5]. Fermi-liquids without disorder at intermediate coupling are invariant [6] under Eq. (1), as are most other contemporary theories of cuprates that I am aware of.

On the other hand two recent theories, the extremely correlated Fermi-liquid theory (ECFL) proposed by the author in Ref. [7], and the hidden Fermi-liquid theory proposed by Casey and Anderson (CA) in Ref. [8], yield a spectral function that lacks invariance under Eq. (1). In Ref. [9], a comparison between the ECFL spectral function and a large set of data at optimal doping shows excellent agreement and provides a useful parametrization of the data. To quantify the asymmetry: for optimally doped cuprates, in an energy range of ± 25 meV around μ , the theories and the fits of Ref. [9] (extrapolated to lower ω) yield an asymmetry ratio \mathcal{R} [defined below Eq. (3)] between $\sim 7\%$ and 10% . Because a large asymmetry makes a

decisive ruling on the allowed theories, we propose the direct experimental measurement of this effect and indicate a procedure for the same.

I first discuss a Fermi symmetrization procedure quite distinct from the symmetrization in Refs. [3,10]. I construct an object $\mathcal{S}_{\mathcal{G}}(\vec{k}, \omega)$ [Eq. (2)] from the observed ARPES intensity and find expressions for this in the Fermi-liquid and the ECFL model. I further show how the momentum dependence of the dipole transition probability and the Fermi-liquid parameter Z_k can be absorbed into the constants.

The $\mathcal{S}_{\mathcal{G}}(\vec{k}, \omega)$ function is detailed for a simplified version of ECFL (SECFL), providing an idealized picture of the predicted asymmetry effect in cuprates. I further discuss a related asymmetry of the tunneling conductance in the normal state, and also the expected angle integrated spectrum. Within the SECFL model, where the quasiparticle peaks are sharp over a large fraction of the zone, these exhibit unusual and possibly measurable features.

Fermi symmetrization.—Our first goal is to formulate a procedure for isolating terms in the spectral function near the Fermi energy that are linear in wave vector and frequency $\sim \xi_k - \omega$ (with $\xi_k = \vec{k} \cdot \vec{v}_{k_{\text{F}}}$) found in the recent work [7]. The ARPES intensity is given in terms of the spectral function within the sudden approximation by the expression $I(\vec{k}, \omega) = M(\vec{k})f_{\omega}\rho_{\mathcal{G}}(\vec{k}, \omega)$, where $M(\vec{k})$ is the dipole transition probability which is expected to be a smooth function of \vec{k} and independent of ω . It also contains the Fermi function for occupied states $f_{\omega} = \{1 + \exp(\beta\omega)\}^{-1}$, a nonsymmetric function of ω . Therefore, we first formulate a Fermi symmetrized object:

$$\mathcal{S}_{\mathcal{G}}(\vec{k}, \omega) \equiv f_{\omega}\bar{f}_{\omega}\rho_{\mathcal{G}}(\vec{k}, \omega) = \frac{1}{M(\vec{k})}\bar{f}_{\omega}I(\vec{k}, \omega), \quad (2)$$

where $\bar{f}_{\omega} = 1 - f_{\omega} = f_{-\omega}$. We may now decompose $\mathcal{S}_{\mathcal{G}}(\vec{k}, \omega)$ under Eq. (1) into its antisymmetric $\mathcal{S}_{\mathcal{G}}^{\text{a-s}}(\vec{k}_{\text{F}}|\vec{k}, \omega)$ and symmetric $\mathcal{S}_{\mathcal{G}}^{\text{s}}(\vec{k}_{\text{F}}|\vec{k}, \omega)$ combinations

respectively $\frac{1}{2}[\mathcal{S}_{\mathcal{G}}(\vec{k}_F + \vec{k}, \omega) \mp \mathcal{S}_{\mathcal{G}}(\vec{k}_F - \vec{k}, -\omega)]$. We will also define the important asymmetry ratio:

$$\mathcal{R}_{\mathcal{G}}(\vec{k}_F|\vec{k}, \omega) = \mathcal{S}_{\mathcal{G}}^{\text{a-s}}(\vec{k}_F|\vec{k}, \omega)/\mathcal{S}_{\mathcal{G}}^{\text{s}}(\vec{k}_F|\vec{k}, \omega), \quad (3)$$

where normalization factors cancel out, giving a dimensionless function of order unity. Its magnitude can therefore be compared across different systems. We will quote $\mathcal{R}_{\mathcal{G}}$ and $\mathcal{S}_{\mathcal{G}}^{\text{s}}$ below for various theoretical models; $\mathcal{S}_{\mathcal{G}}^{\text{a-s}}$ can be reconstructed from Eq. (3).

Dynamical particle-hole symmetry of the Fermi-liquid theory.—We begin by considering $\mathcal{S}_{\mathcal{G}}$ for the Fermi-liquid theory. The spectral function of a Fermi-liquid $\rho_{\mathcal{G}}^{\text{FL}}(\vec{k}, \omega)$ is given in terms of a smooth background plus a quasiparticle peak as in Eq. (4). Near the Fermi surface, we can linearize various objects in \vec{k} and ω . With $\vec{v}_{\vec{k}_F}$, the Fermi velocity vector at \vec{k}_F , the quasiparticle piece is specified by three parameters (i) renormalization factor $Z_{\vec{k}}$, with a linear dependence $Z_{\vec{k}} = Z_{\vec{k}_F}[1 + c_1(\vec{k} \cdot \vec{v}_{\vec{k}_F})]$, (ii) the quasiparticle energy $E_{\vec{k}}$ vanishing linearly at the Fermi surface $E_{\vec{k}} = \frac{m}{m^*}(\vec{k} \cdot \vec{v}_{\vec{k}_F})$ with an effective mass renormalization $\frac{m}{m^*}$, and (iii) the line width $\gamma_{\vec{k}} \propto [E_{\vec{k}}^2 + (\pi k_B T)^2]$ vanishes symmetrically at the Fermi surface. Thus near the Fermi surface:

$$\rho_{\mathcal{G}}^{\text{FL}}(\vec{k}, \omega) \sim \rho_{\mathcal{G}}^{(bg)}(\vec{k}, \omega) + \frac{Z_{\vec{k}}}{\pi} \frac{\gamma_{\vec{k}}}{\gamma_{\vec{k}}^2 + (\omega - E_{\vec{k}})^2}. \quad (4)$$

For \vec{k} close to the Fermi surface, the background part is neglected compared to the large quasiparticle part. Defining the quasiparticle peak part

$$\mathcal{Q}(\vec{k}, \omega) = \frac{Z_{\vec{k}_F}}{4\pi \cosh^2(\beta\omega/2)} \frac{\gamma_{\vec{k}_F}}{\gamma_{\vec{k}_F}^2 + [\omega - \frac{m}{m^*}(\vec{k} \cdot \vec{v}_{\vec{k}_F})]^2}, \quad (5)$$

we write the Fermi symmetrized functions of (\vec{k}, ω) :

$$\{\mathcal{S}_{\mathcal{G}_{\text{FL}}}^{\text{s}}, \mathcal{R}_{\mathcal{G}_{\text{FL}}}\} = \{\mathcal{Q}(\vec{k}, \omega), c_1(\vec{k} \cdot \vec{v}_{\vec{k}_F})\}, \quad (6)$$

where we retained only terms linear in \vec{k} , ω beyond the quasiparticle peak term $\mathcal{Q}(\vec{k}, \omega)$. Observe that to $O(\omega^2)$ the asymmetry ratio \mathcal{R} is independent of ω . The requirement of neglecting the background is necessary, because it is hard to make a general statement about the (k, ω) dependence of the background part. Therefore, the discussion becomes sharp only in situations where the peak term overwhelms the background part—thus, forcing us to low temperatures. The same issue also impacts the synchrotron data adversely compared to the laser ARPES data, if we interpret the former to have more substantial elastic scattering correction as argued in Ref. [9].

We make a few remarks next. (1) The coefficient c_1 vanishes in theories where the self-energy is ω dependent but \vec{k} independent. To the extent that we can experimentally identify a ω independent but k dependent term as in Eq. (6), one can say that the Fermi-liquid spectrum possesses the dynamical particle-hole invariance. (2) The momentum dependence of the dipole transition probability $M(\vec{k})$, if any, can be absorbed into c_1 in Eq. (6) by Taylor expansion. This implies that the expression [Eq. (6)] is valid for the \mathcal{S} , \mathcal{R} constructed from the ARPES intensities directly [i.e., omitting the $1/M$ term in Eq. (2)]. The important asymmetry ratio \mathcal{R} gets rid of the overall scale factors. Therefore, its magnitude is a meaningful quantitative measure of the asymmetry. (3) It follows that the frequency independence of \mathcal{R} is also true for any theory where the Dyson self-energy $\Im m \Sigma(k, \omega)$ is even (i.e., not necessarily quadratic) in ω , such as the marginal Fermi-liquid [11] and also various refinements of the RPA. Subleading corrections of the type $\omega \times T^2$ or ω^3 in $\Im m \Sigma(k, \omega)$ [5], as well as intrinsic particle-hole asymmetric density of states (DOS) terms can lead to a nontrivial \mathcal{R} . However, these are estimated [5,6] to be an order of magnitude smaller than the predicted asymmetry of the theories discussed next.

The asymmetry ratio in ECFL.—In the recent work on the ECFL [7] $\rho_{\mathcal{G}}(\vec{k}, \omega)$ is the product of a Fermi-liquid spectral function $\rho_{\mathcal{G}}^{\text{g}}(\vec{k}, \omega)$ and a caparison factor $[[1 - \frac{n}{2}] + \frac{\xi_{\vec{k}} - \omega}{\Delta(\vec{k}, \omega)} + \eta(\vec{k}, \omega)]$, explicitly containing a linear dependence on the energy ω . This important term redistributes the dynamical spectral weight within the lower Hubbard band, in such a way as to preserve the Fermi volume. In a further approximation of the formalism, a SECFL theory emerges where we obtain explicit analytical results. In this version, $\eta(\vec{k}, \omega)$ is negligible and the coefficient Δ is a constant determined by the number sum rule. In Refs. [9,12], the SECFL was tested against data on the high T_c cuprate $\text{Bi}_2\text{Sr}_2\text{CaCu}_2\text{O}_{8+\delta}$. The test spans a substantial range of occupied energies ~ 1 eV, with quantitative fits in the 0.25 eV energy range. The remarkably close agreement between data and theory over the broad range of data sets appears to vindicate the form of the spectral function. The test proposed in this Letter is somewhat complementary, it is over a smaller energy range $\sim 2k_B T$, probing the asymptotic low energy region centered around the Fermi energy.

With the assumption of a smooth k dependence of $\eta(\vec{k}, 0)$ and $\Delta(\vec{k}, 0)$ in the expression for the spectral function [13] and $p = d_0 + (1 - \frac{n}{2})$, we obtain

$$\mathcal{S}_{\mathcal{G}_{\text{ECFL}}} \sim \mathcal{Q} \left[p + d_1 \vec{k} \cdot \vec{v}_{\vec{k}_F} + d_2 \omega + \frac{(\vec{k} \cdot \vec{v}_{\vec{k}_F} - \omega)}{\Delta(\vec{k}_F)} \right].$$

Here the term d_0 arises from Taylor expanding $\eta(\vec{k}_F, 0)$ and also from the shift of the chemical potential from the

free value, d_1 from the momentum dependence of Z_k and this term can also absorb the momentum dependence of $M(k)$, and d_2 from the frequency dependence of $\eta(k, \omega)$. We can thus compute the symmetric and antisymmetric parts $\{\mathcal{S}_{\mathcal{G}_{\text{ECFL}}}^s, \mathcal{R}_{\mathcal{G}_{\text{ECFL}}}\}$ as

$$\sim \left\{ p\mathcal{Q}, \frac{d_1}{p} \vec{k} \cdot \vec{v}_{\vec{k}_F} + \frac{d_2}{p} \omega + \frac{(\vec{k} \cdot \vec{v}_{\vec{k}_F} - \omega)}{p\Delta(\vec{k}_F)} \right\}. \quad (7)$$

The asymmetry ratio \mathcal{R} therefore has a linear ω and \hat{k} dependence. Using the frequency dependence as the signature, one should be able to distinguish between the results of Eqs. (6) and (7).

The SECFL model is described in detail in Ref. [12], where we write the spectral function near the Fermi energy $\rho_{\mathcal{G}_{\text{SECFL}}}^{\text{Peak}}(\vec{k}_F + \vec{k}, \omega)$ as

$$\frac{1}{\pi} \frac{Z_k^2 \Gamma_k}{Z_k^2 \Gamma_k^2 + (\omega - E_k^{\text{FL}})^2} \frac{n^2}{4\Delta_0} \{\varepsilon_0 + \xi_k - \omega\}, \quad (8)$$

where $\varepsilon_0 = \Delta_0 \frac{4}{n^2} (1 - \frac{n}{2})$. Here $E_k^{\text{FL}} = Z_k \xi_k$, in view of the form of the self-energy Φ . To leading order, we can set $Z_k \rightarrow Z_F$ independent of k , and $\xi_k = \vec{k} \cdot \vec{v}_{\vec{k}_F}$, $E_k^{\text{FL}} = Z_F \vec{k} \cdot \vec{v}_{\vec{k}_F}$, and set $\Gamma_k = \eta + \pi C_\Phi [(\pi k_B T)^2 + (E_k^{\text{FL}})^2]$, where η is the elastic broadening introduced in Ref. [9] [distinct from $\eta(\vec{k}, \omega)$]. For the model Eq. (8), we can set $\Gamma_k \rightarrow \Gamma_{k_F}$ and thus obtain the leading behavior near the Fermi energy of $\{\mathcal{S}_{\mathcal{G}_{\text{SECFL}}}^s, \mathcal{R}_{\mathcal{G}_{\text{SECFL}}}\}$ as

$$\sim \left[\left(1 - \frac{n}{2}\right) \mathcal{Q}(\vec{k}, \omega), \frac{\{\vec{k} \cdot \vec{v}_{\vec{k}_F} - \omega\}}{\varepsilon_0} \right], \quad (9)$$

where $\mathcal{Q}(\vec{k}, \omega)$ is obtained from Eq. (5) by replacing $m/m^* \rightarrow Z_F$ and $\gamma_k \rightarrow \Gamma_k Z_k$. Note that, e.g., at $\vec{k} = \vec{0}$ and any convenient ω_0 , $|\mathcal{R}(0, \omega_0)| = \omega_0/\varepsilon_0$, and thus its magnitude yields the important energy scale Δ_0 . We emphasize that Eq. (7) is more generally true within the ECFL approach. We display $\mathcal{S}^{\text{a-s}}$ in Fig. 1 for a model calculation based in the SECFL model with a flat DOS [see Ref. [12], Sec. (IV.F)]. The values of the basic parameters in all figures are as follows: $T = 180$ K, $\omega_c = 0.25$ eV, $C_\Phi = 1$ (eV) $^{-1}$. Notice the distinctive increasing linear behavior with \vec{k} and a decreasing linear one with ω , as in Eqs. (7) and (9).

Single particle tunneling into the extremely correlated state.—In the simplest model of tunneling in the t - J model, the conductance is given in terms of the local DOS $\rho_{\mathcal{G}}^{(\text{local})}(\omega) = \sum_{\vec{k}} \rho_{\mathcal{G}}(\vec{k}, \omega)$. Its convolution with f_ω and \bar{f}_ω gives half the occupied $\frac{n}{2}$, and the unoccupied $(1 - n)$ densities, thus providing useful sum rules for tunneling [14]. The sum rule implies asymmetry between adding particles and holes and thus a downward sloping conductance [15, 16]. Recent experiments in the overdoped regime

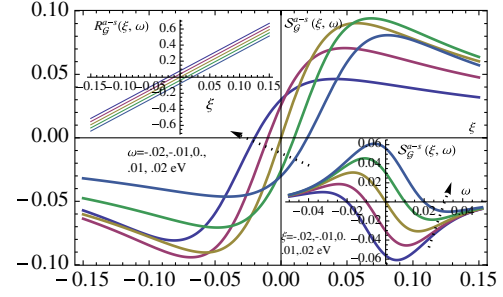


FIG. 1 (color online). Top inset shows the large predicted asymmetry $\mathcal{R}_{\mathcal{G}_{\text{SECFL}}}^{\text{a-s}}$ versus ξ in the small energy range of 150 meV. Similar magnitudes are found as functions of ω at various ξ . The figure shows $\mathcal{S}_{\mathcal{G}_{\text{SECFL}}}^{\text{a-s}}$ from Eq. (9) versus ξ (main), ω (inset) in electron volt at various ω (main), ξ (inset). Arrows indicate the direction of increasing energies. We used $n = 0.85$, $\eta = 0.05$ eV, and $\Delta_0 = 0.0796$ eV here.

[17, 18] display the same asymmetry, providing strong confirmation that t - J model type extreme correlations are operative at high hole doping levels as well, and not just near half filling. More detailed information on the frequency dependence is clearly of experimental interest. We note that the angle integrated photo emission (AIP) technique obtains the local DOS $\times f_\omega$, and provides a complementary view to tunneling. Figure 2 presents the results from the SECFL model for both the (local) DOS and DOS $\times f_\omega$ at various densities and elastic scattering parameter η . It shows an overall decrease of the local DOS with energy. Interestingly, the tunneling curve in the inset (III) shows an upturn followed by a rising piece near $\omega \sim 0$, and the AIP curve shows a related shallow minimum at $\omega \sim -0.2$ eV.

To understand the unusual result, consider integrating the spectral function in Eq. (8) over ξ_k . As discussed in Refs. [9, 12], when the energy is less than ~ 1 eV, the quasiparticles become sharp and this integral can be

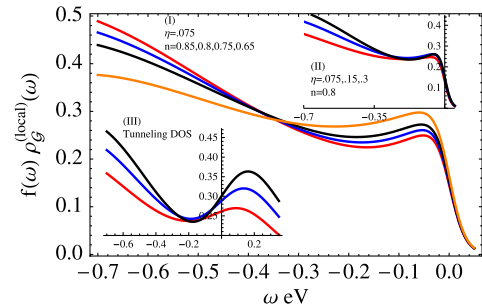


FIG. 2 (color online). (I) The predicted AIP spectrum showing a shallow minimum at $\omega \sim -0.2$ eV, and a rise as the binding energy $|\omega|$ increases. The rise is greater as the particle density n increases (bottom to top). Inset (II) reveals the role of elastic scattering width η (top to bottom). Inset (III) shows the local DOS relevant to the tunneling conductance, for the same parameters as in (II) with a remarkable rising piece near zero bias.

estimated by replacing the Fermi-liquid Lorentzian by $\delta(\vec{k} \cdot \vec{v}_{\vec{k}_F} - \frac{m^*}{m}\omega)$. This yields the quasiparticle peak contribution:

$$\lim_{\omega \rightarrow \varepsilon_0} \rho_{G, \text{Peak}}^{(\text{local})}(\omega) \sim \text{const} \times \left\{ \varepsilon_0 + \left(\frac{m^*}{m} - 1 \right) \omega \right\}. \quad (10)$$

Because $m \leq m^*$, it follows that the slope is positive and hence the rising conductance! In the general version of ECFL, different parts of the Fermi surface contribute according to the weight of $1/\Delta(\vec{k}_F)$. We expect the resulting average to be less favorable to a rising term than in the SECFL model.

Other theories.—CA in Ref. [8] provide a spectral function that may be Taylor expanded at finite T and low enough energies as follows. With $q = 1 - \frac{1}{4}n^2$ depending on the filling n , and $\Gamma_{\hat{k}} = A(k_B T) + C v_{\vec{k}_F}^2 \hat{k}^2$, their expressions yield:

$$\{\mathcal{S}_{CA}^s, \mathcal{R}_{CA}^{a-s}\} = \left\{ \mathcal{Q}', \cot(q\pi/2) \frac{(v_F \hat{k} - \omega)}{\Gamma_0} \right\}, \quad (11)$$

with $\mathcal{Q}' = \text{const} \times \frac{\sin(q\pi/2)}{4\pi \cosh^2(\beta\omega/2)} / [\Gamma_0^2 + (\omega - v_F \hat{k})^2]^{q/2}$. Therefore, this work also implies a nontrivial \mathcal{R} with a linear ω , \hat{k} dependence, similar in form to that in ECFL, although with a non-Lorentzian peak factor replacing the \mathcal{Q} factor in Eq. (7). It is seen that the asymmetry of this theory as well as that of the ECFL theory vanishes continuously at low particle density $n \rightarrow 0$. An important characteristic energy $\Delta^*(x, T)$, say the inverse of the slope of the linear in ω term in \mathcal{R} contains much physics. In the CA theory $\Delta^*(x, T) \propto \Gamma_0$ vanishes at all densities x as $T \rightarrow 0$, thereby defining a line of quantum critical points. On the other hand in the ECFL calculations, the energy $\Delta^*(x, T \rightarrow 0)$ is nonzero but much smaller than the (bare) Fermi energy. However, it could vanish at a specific filling x_c : as $\Delta^*(x_c, T \rightarrow 0) \rightarrow 0$, thereby locating an isolated quantum critical point.

Other contemporary theories have a different prediction from the ECFL and CA. The popular marginal Fermi-liquid model [11] for the spectral function has a Dyson self-energy that is symmetric under the transformation Eq. (1). Therefore, it leads to an ω independent asymmetry ratio at small energies, as in the usual Fermi-liquid [6]. A similar ω independent \mathcal{R} occurs for the RPA and its many variants emphasizing fluctuation contributions.

Conclusions.—The program of extraction of the asymmetry ratio from the “ideal” spectral weight is summarized in Fig. 3. A window of size $\sim 2k_B T$ in ω and $v_F \hat{k}$ are highlighted in this construction. It is proposed that a careful examination of the ARPES intensity along these lines would determine the existence of dynamical particle-hole asymmetry. This asymmetry also relates to the difference in velocities (and amplitudes) of quasiparticles and quasiholes, of the type that are invoked in explaining the

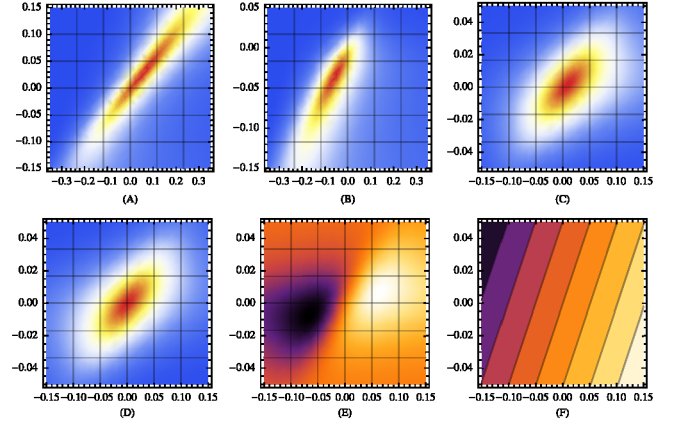


FIG. 3 (color online). Symmetry extraction illustrated for the simplified ECFL model. Here $n = 0.85$, $\eta = 0.05$, and $\Delta_0 = 0.0796$ with ω (ordinate) and ξ (abscts antisymmetricissa) in electron volt. (A) Shows the spectral function ρ_G , (B) $\rho_G f_\omega$, (C) $\rho_G f_\omega f_\omega$, (D) the symmetrized object \mathcal{S}_G^s , (E) the antisymmetrized object \mathcal{S}_G^{a-s} showing a peak and a trough, and (F) the asymmetry ratio \mathcal{R}_G from Eq. (3).

peculiar sign of the Hall effect in the mixed state [19]. We thus expect it to be important in Hall and analogous transport contexts such as thermopower. This search is complementary, as well as a prerequisite, to the detailed characterization of the symmetric part \mathcal{S}^s . Specifically I propose that the search for a nontrivial (i.e., ω linear) asymmetry ratio \mathcal{R} is important for identifying the correct underlying theoretical description of the cuprates.

In order to implement the transformation Eq. (1) on the experimental data, we need a high resolution in frequency as well as momentum. Because the bare Fermi velocities are high $\hbar v_F \sim 5 \text{ eV \AA}$, the momentum resolution becomes critical. An error $\Delta \xi \sim 15\text{--}20 \text{ meV}$ can lead to quite incorrect conclusions. Thus, in order to draw unambiguous conclusions we require $\Delta k \sim 0.001 (\text{\AA})^{-1}$, i.e., $\Delta \xi \sim 5 \text{ meV}$ or better, thereby posing an interesting challenge to the experimental ARPES community.

This work was supported by DOE under Grant No. FG02-06ER46319. I thank A. Chubukov, A. Georges, G. H. Gweon, D. Huse, H. R. Krishnamurthy, and T. V. Ramakrishnan for stimulating comments.

- [1] C. P. Herzog, P. Kovtun, S. Sachdev, and D. T. Son, *Phys. Rev. D* **75**, 085020 (2007); T. Senthil, *Phys. Rev. B* **78**, 035103 (2008).
- [2] S. S. Lee, *Phys. Rev. D* **79**, 086006 (2009).
- [3] M. Norman *et al.*, *Nature (London)* **392**, 157 (1998); M. R. Norman, M. Randeria, H. Ding, and J. C. Campuzano, *Phys. Rev. B* **57**, R11093 (1998); M. R. Norman, H. Ding, H. Fretwell, M. Randeria, and J. C. Campuzano, *Phys. Rev. B* **60**, 7585 (1999); U. Chatterjee *et al.*, *Proc. Natl. Acad. Sci. U.S.A.* **108**, 9346 (2011).

- [4] J. Schmalian and C. D. Batista, *Phys. Rev. B* **77**, 094406 (2008).
- [5] C. Hodges, H. Smith, and J. W. Wilkins, *Phys. Rev. B* **4**, 302 (1971) find a small (odd in ω) correction to the usual ω^2 behavior $\Sigma'' \propto \omega^2(1 - \frac{2}{3}\omega/\varepsilon_f)$.
- [6] A small asymmetry is inevitably induced by DOS variation leading to an estimated asymmetry ratio \mathcal{R} [Eq. (3)] that is an order of magnitude smaller than that found in the ECFL and CA theories. Also the unavoidable disorder contributes, and thus one may operationally refer to cases as essentially invariant if $|\mathcal{R}| \leq 1\%$ in an energy window of ± 25 meV around μ .
- [7] B. S. Shastry, *Phys. Rev. Lett.* **107**, 056403 (2011).
- [8] P. A. Casey and P. W. Anderson, *Phys. Rev. Lett.* **106**, 097002 (2011); P. A. Casey, J. D. Koralek, N. C. Plumb, D. S. Dessau, and P. W. Anderson, *Nature Phys.* **4**, 210 (2008); P. W. Anderson, *Nature Phys.* **2**, 626 (2006); S. Doniach and M. Sunjic, *J. Phys. C* **3**, 285 (1970).
- [9] G.-H. Gweon, B. S. Shastry, and G. D. Gu, *Phys. Rev. Lett.* **107**, 056404 (2011).
- [10] The Fermi symmetrization defined in Eq. (2) corrects for the asymmetry of $I(\omega)$ arising from f_ω , by multiplying with \bar{f}_ω . The term symmetrization of Ref. [3] refers to a different procedure. At the Fermi momentum, Ref. [3] assumes that $\rho_G(\omega) = \rho_G(-\omega)$. Under this assumption, the authors argue that $I(\omega) + I(-\omega) \rightarrow \rho_G(\omega)M(\vec{k}_F)$. The asymmetry ratio \mathcal{R} of Eq. (3) in this case is $([\bar{f}_\omega I(\omega) - f_\omega I(-\omega)]/[f_\omega I(\omega) + \bar{f}_\omega I(-\omega)])$ and vanishes under their assumption.
- [11] C. M. Varma, P. B. Littlewood, S. Schmitt-Rink, E. Abrahams, and A. E. Ruckenstein, *Phys. Rev. Lett.* **63**, 1996 (1989).
- [12] B. S. Shastry, *Phys. Rev. B* **84**, 165112 (2011).
- [13] The energy variables $\Delta(\vec{k}, \omega)$ and $\eta(\vec{k}, \omega)$ are defined in Eqs. (21–23) of Ref. [7].
- [14] M. Randeria, R. Sensarma, N. Trivedi, and F. C. Zhang, *Phys. Rev. Lett.* **95**, 137001 (2005).
- [15] P. W. Anderson and N. P. Ong, *J. Phys. Chem. Solids* **67**, 1 (2006).
- [16] T. Hanaguri, C. Lupien, Y. Kohsaka, D.-H. Lee, M. Azuma, M. Takano, H. Takagi, and J. C. Davis, *Nature (London)* **430**, 1001 (2004).
- [17] A. Pasupathy, A. Pushp, K. Gomes, C. Parker, J. Wen, Z. Xu, G. Gu, S. Ono, Y. Ando, and A. Yazdani, *Science* **320**, 196 (2008), Figs. 4A, 1A, 1B.
- [18] C. Renner, B. Revaz, J. Y. Genoud, K. Kadowaki, and O. Fischer, *Phys. Rev. Lett.* **80**, 149 (1998).
- [19] J. M. Harris, N. P. Ong, and Y. F. Yan, *Phys. Rev. Lett.* **71**, 1455 (1993); A. T. Dorsey, *Phys. Rev. B* **46**, 8376 (1992).